VCST Internal Memo

Title: Assessment of FP-11 Polarization Sensitivity for the JPSS-2 VIIRS VisNIR Bands and DNB
Memo Number: 2017_011
Revision: 01
Date: May 11, 2017
Author: Jeff McIntire
To: Xiaoxiong Xiong and James Butler
Cc: Hassan Oudrari, Kwo-Fu (Vincent) Chiang, and Aisheng Wu

References

[1] TP1544640-2222 Rev A, 'Polarization Sensitivity FP-11 Test Procedure,' Raytheon.
[2] VCST_TECH_REPORT_16_026, 'Preliminary Analysis of JPSS-2 FP-11 Polarization Sensitivity Data,' Jeff McIntire, July 22, 2016.
[3] J2 pol analysis20160722 by test, Raytheon, July 22, 2016.
[4] J2 pol analysis20160722 by band, Raytheon, July 22, 2016.
[5] VCST_TECH_MEMO_14_002, 'Assessment of FP-11 Polarization Sensitivity for the VIIRS F2 VisNIR Bands,' Jeff McIntire, March 13, 2014.
[6] VCST_TECH_MEMO_14_005, 'Estimate of Uncertainty in FP-11 Polarization Sensitivity Measurements for the VIIRS F2 VisNIR Bands,' Jeff McIntire, April 9, 2014.
[7] VCST_TECH_MEMO_14_007, 'Assessment of FP-11 Polarization Sensitivity for the VIIRS F2 DNB LGS,' Jeff McIntire, April 11, 2014.
[8] VCST_TECH_MEMO_15_002, 'Assessment of FP-11' Polarization Sensitivity for the JPSS J1 VIIRS VisNIR Bands and Comparison to FP-11 Measurements,' Jeff McIntire, February 12, 2015.
[9] VCST_TECH_MEMO_15_005, 'Assessment of FP-11' Polarization Sensitivity for the JPSS J1 VIIRS DNB LGS,' Jeff McIntire, March 2, 2015.
[10] VCST_TECH_MEMO_15_015, 'Updated Estimate of Uncertainty in FP-11 and FP-11' Polarization Sensitivity Measurements for the JPSS J1 VIIRS VisNIR Bands,' Jeff McIntire, September 1, 2015.
[11] VIIRS PRD Rev C, 'Joint Polar-orbiting Satellite System (JPSS) Visible Infrared Imaging Radiometer Suite (VIIRS) Performance Requirements Document (PRD).'
[12] VIIRS.10.15.075, 'J2 VIIRS Polarization Test Source Assembly (PTSA) Calibration and Performance Verification,' Tung Wang, Tim P Johnson, and Dan Tiffany, February 2, 2016.
[13] Mathematical Methods in the Physical Sciences, Mary L. Boas, John Wiley & Sons, 1985.
[14] 'VIIRS Polarization Sensitivity Analysis,' Eric C. Fest, Page E. King, and Steve J. Herbst, Raytheon, February 10, 2014.
[15] An Introduction to Error Analysis, John R. Taylor, University Science Books, 1997.

1. Introduction

JPSS-2 VIIRS sensor polarization sensitivity was measured for the VisNIR bands and DNB during FP-11 in ambient testing [1]. Preliminary NASA analysis was reported in [2] and Raytheon reported their results in [3-4]. This work will provide an overview of the test setup and objectives, analysis methodology, and results as well as a comparison to earlier JPSS-1 and SNPP VIIRS measurements [5-10].

2. Objective

The objective of the FP-11 test was to determine the sensitivity of the VIIRS instrument to input linearly polarized light. There are two specifications which relate to the polarization sensitivity of VIIRS [11]:

> **V_PRD-12624** – The VIIRS Sensor linear polarization sensitivity of the VIS and NIR bands shall be less than or equal to the values indicated in Table 1 for scan angles less than 45 degrees off Nadir.
>
> **V_PRD-12667** – The VIIRS Sensor linear polarization sensitivity shall be measured within a characterization uncertainty of 0.5% (one sigma) for scan angles less than 55.84 degrees off Nadir.

Both specifications will be addressed in this memo.

2. Test Equipment

The Polarization Test Source Assembly (PTSA) was used to measure the polarization sensitivity of the JPSS-2 VIIRS sensor [12]. This setup consisted of an integrating sphere, polarizer sheets, shaping filters, and various baffling [12]. VIIRS was placed on a rotating mount such that the angle at which VIIRS viewed the PTSA could be varied. The PTSA was viewed at the following VIIRS scan angles: -55, -45, -37, -30, -20, -15, -8, 4, 22, 45, and 55 degrees. A general schematic of the test setup is shown in Figure 1 indicating the placement of the filters and polarizers relative to the path. Figure 2 references the polarizer angle to VIIRS coordinates system including the rotation of the polarizer (in this figure, the view is from VIIRS through the polarizer to the integrating sphere).

An integrating sphere (SIS-100-2) was used as a source for FP-11 testing. The SIS-100-2 is a 100 cm integrating sphere with a 12 inch circular aperture. The lamp configurations used during testing were BH and CJ; each letter represents a different 600 W bulb. Testing began with lamp configuration BH, However, radiance monitor data showed that this lamp configuration started to drift part way through the test sequence, as shown in Figures 3 and 4. It was decided to switch to lamp configuration CJ and recollect some of the affected data. Spectra for similar lamp configurations used during JPSS-1 VIIRS testing are plotted in [8].

Two polarization sheet used during testing: BVONIR and BVO777. The polarizers were mounted on a rotary stage which could be cycled from 0 and 360 degrees. A second fixed polarizer of the same type was used in conjunction with the first to measure the polarizer efficiency. The degree of linear polarization for the BVONIR polarizer is plotted in [8].

The shaping filter used during testing was the Sonoma filter. The Sonoma filter is a long wave blocking filter with very low transmittance above about 650 nm. The transmittance of the shaping filter is plotted in [8]. In addition, the convolution of this transmittance with the source spectra using during JPSS-1 VIIRS testing as well as the TOA spectra are plotted in [8].

In addition, a lollipop obscuration was inserted into the optical path (preceding the polarizer, but after the Sonoma filter) to investigate possible stray light contamination.

3. Test Configuration

Four test configurations were used during FP-11 testing: BVONIR with the Sonoma filter, BVONIR without the Sonoma filter, BVO777 with the Sonoma filter, and BVO777 without the Sonoma filter.

Stray light, efficiency, and polarization sensitivity tests were performed for both BVONIR configurations; for the BVO777 configurations, efficiency and polarization sensitivity data were only collected once at the -8 degree scan angle to provide continuity with SNPP and JPSS-1 VIIRS sensors. Testing with the Sonoma filter used 80 % of nominal integration time for the M bands and testing without the Sonoma filter used 6 % of nominal integration time (testing on JPSS-1 VIIRS used two different lamp levels).

First, a stray light investigation was performed for the BVONIR configurations by performing two tests: one with the source off and the room dark, and the other with the source on and a lollipop obscuration inserted into the path. The rotating polarizer was then cycled through 25 different angles from 0 to 360 degrees in 15 degree increments for both tests.

Next, a second fixed polarizer was inserted into the path between the rotating polarizer and VIIRS for all four configurations. The rotating polarizer was then cycled through 25 different angles from 0 to 360 degrees in 15 degree increments.

Lastly, the polarization sensitivity of VIIRS instrument was measured for all four configurations. The BVONIR configurations were measured at all 11 scan angles including three repeated measurements at -8 degrees. The configurations with the Sonoma filter were used to measure the sensitivity of bands M1 – M3, while the sensitivity of bands I1 – I2 and M4 – M7 was measured without the Sonoma filter. However, useful data was collected for some bands in both configurations (with and without the Sonoma filter). The BVO777 configurations were measured only at -8 degrees scan angle. This work will focus on the BVONIR results.

4. Methodology

A standard Fourier analysis was used to determine the polarization sensitivity of the VIIRS instrument [13]. The Fourier expansion is written as

$$dn = \frac{1}{2}c_0 + \sum_n c_n \cos(n\theta) + \sum_n d_n \sin(n\theta), \tag{1}$$

where the Fourier coefficients are defined by the following:

$$c_n = \frac{1}{\pi}\int_{-\pi}^{\pi} \cos(n\theta)\, dn(\theta)\, \partial\theta, \tag{2}$$

and

$$d_n = \frac{1}{\pi}\int_{-\pi}^{\pi} \sin(n\theta)\, dn(\theta)\, \partial\theta. \tag{3}$$

In this work, only the zeroth through fourth order Fourier coefficients were calculated (for the polarizer efficiency tests, only the zeroth and second order terms were calculated). Eq. (1) can be rewritten as

$$dn = \frac{1}{2}c_0\left[1 + \sum_{n=1}^{4} a_n \cos(n\theta - \delta_n)\right], \tag{4}$$

where the linear polarization sensitivity of the instrument (referred to below as the polarization factor) is defined as

$$a_n = \frac{\sqrt{c_n^2 + d_n^2}}{\frac{1}{2}c_0\sqrt{a_2^{eff}}} \tag{5}$$

and the phase angle is defined as

$$\delta_n = \tan^{-1}\left(\frac{d_n}{c_n}\right). \qquad (6)$$

The efficiency of the polarizer is defined as

$$a_2^{eff} = \frac{\sqrt{c_2^2 + d_2^2}}{\frac{1}{2}c_0}, \qquad (7)$$

and was determined from the cross polarizer testing.

5. Uncertainty Estimate

5.1 dn Uncertainty

The uncertainty on the dn used in this work consists of three sources: noise, source stability, and stray light.

The random noise associated with each measurement is determined by the standard deviation of the mean over all samples and scans used at a particular polarizer angle:

$$u = \sigma_m . \qquad (8)$$

The source stability was estimated by taking the difference of repeated measurements. The polarizer sheet was rotated from 0 to 360 degrees in 15 degree increments; for a given polarizer angle θ, θ and θ+180 are repeated measurements. Each pair of measurements was used to generate the source stability contribution to the dn uncertainty for that pair of measurements:

$$u = \left|dn(\theta) - dn(\theta + 180)\right| . \qquad (9)$$

Here the dn is sensor response averaged over all available scans and samples.

The stray light was determined from the separate stray light testing using the lollipop obscuration. The measured stray light forms a pedestal that increases the zeroth order Fourier coefficient (assuming no modulation with polarizer angle) and as such constitutes a bias uncertainty:

$$u = \max[dn(lollipop)]. \qquad (10)$$

It was not removed in the processing as the stray light was observed to be 0.1 – 0.2 dn for the majority of detectors.

5.2 Polarizer Angle Uncertainty

The polarizer sheet transmittance axis was aligned with the VIIRS RTA rotation axis. To estimate the alignment uncertainty, a cross polarizer was used to determine the deviation of the angle of maximum transmittance from the expected angle; since we expect a cos(2θ) curve, the uncertainty is

$$u = \left|\delta_2 / 2\right| , \qquad (11)$$

where δ_2 is the two cycle phase angle.

5.3 Repeatability Uncertainty

The polarization sensitivity measurements were conducted three times at -8 degrees scan angle. The range of calculated values for the polarization factor was used as an uncertainty on the repeatability of the measurement, or

$$u = \left|\max\left[a_2(-8)\right] - \min\left[a_2(-8)\right]\right|. \tag{12}$$

5.4 Scan Angle Interpolation Uncertainty

Measurements of the polarization sensitivity were made at 11 discrete scan angles (-55, -45, -37, -30, -20, -15, -8, 4, 15, 22, 45, and 55 degrees). However, the sensitivity needs to be known at all scan angles. The average residual of a quadratic polynomial fit to the measurements is used to estimate the uncertainty due to scan angle interpolation, or

$$u = mean(residual). \tag{13}$$

5.5 SIS – TOA Uncertainty

Modeling of the transmittance of linearly polarized light has shown that the bulk of the sensitivity derives from the differences in transmittance to input polarized light at the edges of the bandpasses, especially for bands M1 – M4 [14]. As a result, the uncertainty due to differences in the source spectra from the TOA radiance needs to be included. Four input polarization states were modeled (0, 45, 90, and 135 degrees). The modeled transmittance was provided for bands M1 – M7, detectors 1, 4, 8, 12, and 16, at all seven measured scan angles. These transmittances were convolved with the input spectra, and the modeled polarization factor was derived. The modeled polarization factors for the SIS and TOA spectra are shown in [8]. The maximum difference between the two per band is used as the uncertainty, or

$$u = \max\left|a_{2-\mathrm{mod}el}(SIS) - a_{2-\mathrm{mod}el}(TOA)\right|. \tag{14}$$

Note that the model used here was not HAM dependent. These results were then linearly interpolated to all detectors and scan angles measured. Band M7 data was used for band I2 and limited band I1 at -8 degrees scan angle was used for all measurements.

5.6 OOB Uncertainty

The SIS – TOA uncertainty described above for bands M1 – M7 considered only in-band effects on the polarization sensitivity. The out-of-band (OOB) could also vary with input polarized light. To estimate the potential OOB impact, the measurements with and without the Sonoma filter were compared:

$$u = \left|a_2(SIS/Sonoma) - a_2(SIS)\right|. \tag{15}$$

However, this uncertainty is only determined here for bands M1 – M3. The other bands had either saturated, had very low signal, or the Sonoma filter excluded only part of the bandpass for one of the test configurations.

5.7 Test Setup Uncertainty

The test setup uncertainty was derived by Raytheon [3,4] and is listed per band in Table 8.

5.8 Uncertainty Propagation

The uncertainty propagation follows the methodology outlined in [15]. The uncertainty tree is shown in Figure 5. First, the dn and sheet angle uncertainties were propagated through the Fourier coefficients calculated from the cross polarizer testing and then used to determine the polarizer DoLP uncertainty. Next, the dn and sheet angle uncertainties were propagated through the Fourier coefficients calculated from the polarization sensitivity testing and combined with the polarizer DoLP uncertainty to determine the measurement uncertainty on the polarization factor. This measurement uncertainty is then RSSed with the following uncertainties: repeatability, scan angle interpolation, SIS – TOA, OOB, and test setup. The final uncertainty is then compared to the specification [11].

6. Analysis

The data analyzed during the FP-11 testing is listed in Tables 2 – 5 (including the type of test, number of collects, scan angle, samples used, and lamp configuration). In this work, 20 EV samples were used in the processing for the M bands (40 samples for the I bands and 20 samples for the DNB LGS). The sample window was chosen to minimize the stray light observed in the lollipop obscuration test and a centroid of the source profile was used to capture the same portion of the source for all scan angles. The OBC BB view data was used as a dark reference, averaged per scan, and subtracted from each EV pixel of the corresponding scan. Then all EV pixels were first averaged over a particular scan and then all scans were averaged in each collect (a 3-sigma outlier rejection was used in each average). Note that the BB data was first truncated from 14 to 12 bits in order to remove any bias between the EV and BB data.

Each collect corresponded to a measurement at a discrete polarizer sheet angle. The angle was cycled from 0 to 360 degrees in 15 degree increments. This set of 25 measurements was then used to determine the Fourier coefficients in Eqs. (2) and (3), and finally the linear polarization sensitivity and phase from Eqs. (5) and (6). The cross polarizer efficiency test was analyzed first; then the efficiency correction defined by Eq. (7) was used in the final polarization sensitivity calculation.

7. Results

Data from the stray light tests was analyzed for both configurations for the dark and lollipop tests. The stray light observed for all detectors in band M7 is shown in Figures 6 (dark) and 7 (lollipop) using the BVONIR polarizer without the Sonoma filter. The stray light observed in the dark configuration is consistent with zero. Some small positive signal was recorded using the lollipop configuration (less than ~0.2 dn for all detectors). All other bands showed similar results (all detectors less than ~0.2 dn). Ideally, any stray light would constitute a pedestal that would need to be subtracted from the polarization sensitivity measurements; however, given the low levels of stray light observed, no additional processing was conducted.

Cross polarizer test data was analyzed for both configurations and the DoLP of the polarizers in each configuration was determined. The efficiency was calculated for each band, detector, and HAM side; the band average results for the BVONIR polarizer with and without the Sonoma filter are shown in Figure 8 (also averaged over HAM side). Note that there is good agreement between the measurements for M1 – M4; the signal is much lower for these bands without the Sonoma filter, and so the efficiency is less well determined for that measurement. Also, the Sonoma filter blocks part of the in-band I1 radiance; as a result, the efficiencies for the different configurations are not consistent. For the remaining bands, the signal with the Sonoma filter was too low to reliably determine the DoLP.

The polarization sensitivity was derived for all VisNIR bands, detectors, HAM sides, and 11 scan angles. Figure 9 plots the measured dn for band M7, HAM side 0 using the BVONIR polarizer without the Sonoma filter at a scan angle of -8 degrees (UAID 4400842). The lines indicate the calculated Fourier series using the zeroth through fourth order terms; the Fourier series reproduces the observed behavior very well. Note that the amplitude and phase of the Fourier series varies with detector. Figure 10 shows the zeroth through fourth order Fourier coefficients for M7, HAM side 0 versus scan angle for all detectors. The zeroth and second order terms are the dominant results (note that the offset trend changed when the lamp configuration changed). There is also a small but non-negligible contribution from the first order term, indicating that there was some minor source instability or drift. The results shown in Figures 9 and 10 are indicative of all VisNIR bands. Figure 11 compares the second order term a_2 across repeated measurements at a scan angle of -8 degrees (band M1, HAM side 0, BVONIR polarizer with the Sonoma filter). The repeated measurements at -8 degrees generally agree well for each BVONIR configuration. The results shown in Figure 11 are representative of all VisNIR bands; the maximum difference between the three repeated measurements (over bands, detectors, and HAM sides) is less than 0.06 %.

The final polarization factors (a_2) are shown for all VisNIR bands, detectors, and scan angles in Figure 12 (13) for HAM side 0 (1). The maximum values per band and scan angle are shown in Table 6 (7) for HAM side 0 (1). The final polarization results were derived using the BVONIR with the Sonoma filter for M1 – M3 and without the Sonoma filter for I1 – I2 and M4 – M7. The first specification in Section 2 applies directly to a_2 for scan angles less than 45 degrees off nadir. For most scan angle – detector combinations, band M1 is non-compliant with the specification (up to ~ 4.8 % for M1). The HAM side dependence is much smaller than observed for JPSS-1 VIIRS with up to about 0.13 % difference compared to up to 1.0 % for JPSS-1. Also, note that there is considerable variation both with detector and with scan angle (up to ~2 % for M1), although this is also much smaller than observed for JPSS-1 VIIRS. The SNPP and JPSS-1 VIIRS maximum a_2 are also listed in Tables 6 and 7 for comparison [5,8]; note that for almost all cases, JPSS-1 has larger polarization sensitivity than SNPP and JPSS-2, while JPSS-2 is comparable to SNPP or smaller with the exception of band M1. The corresponding final polarization phases (δ_2) are shown for all bands, detectors, and scan angles in Figure 14 (15) for HAM side 0 (1). The phase determination becomes difficult when a_2 is small, as a small change in the c_2 or d_2 causes a large change in δ_2 when c_2/d_2 approaches 0 or 1.

The final polarization factors (a_2) for the DNB LGS are shown for all detectors and scan angles in Figure 16 (17) for HAM side 0 (1) for both test configurations. The maximum values per HAM side and scan angle are shown in Tables 6 and 7; the final polarization results were derived using the BVONIR polarizer without the Sonoma filter. For some scan angle – detector combinations, the final DNB LGS polarization factors are as high as ~1.8 %. The HAM side dependence is in general small. The differences between test configurations vary considerably with scan angle and detector; the detector dependence with scan angle is fairly consistent without the Sonoma filter but shows much more variation with the Sonoma filter. The corresponding final polarization phases (δ_2) are shown for all detectors and scan angles in Figure 18 (19) for HAM side 0 (1). Note that the Sonoma filter suppresses the red side of the DNB bandpass, and it was established that the polarization sensitivity varies considerable with wavelength, so the difference in the results of the two configurations is unsurprising.

The final, maximum uncertainties on the polarization factors a_2 per band over detector, HAM side, and scan angle are listed in Table 8 along with the individual uncertainty contributors (in %). Note that the uncertainty contributors highlighted in red were derived for JPSS-1 VIIRS; current estimates from Raytheon for JPSS-2 VIIRS are not yet available. The total uncertainties range from 0.11 % for M6 to 0.43 % for M1; this is comparable to the uncertainty estimates derived for JPSS-1 VIIRS [10]. The specified maximum allowed uncertainty is 0.5 %; all bands are well under this limit. The largest contributors are the source stability, efficiency, SIS – TOA, and test setup uncertainties (note that the SIS-TOA and test setup uncertainties used here were derived for JPSS-1 VIIRS). In particular, the SIS – TOA uncertainty for M1 is by far the single largest contributor for any band at 0.39 %. Source stability was also an issue for bands I1, M4, and M5, as observed by the small but non-negligible one cycle Fourier components.

Note that some of the contributors that are considered biases (stray light and sheet angle uncertainties) enter into the calculation of the uncertainty in the efficiency and also in the measurement total; any possible correlations between these contributions were not considered here. However, these contributions were in general subdominant, and so the overall conclusions are expected to hold.

7. Summary

FP-11 polarization sensitivity testing was performed under ambient conditions for JPSS-2 VIIRS sensor. Analysis showed the following:

- Linear polarization sensitivity for band M1 was observed to be higher than the specified limit (as high as ~4.8 %). All other bands were well within the required limits.
- Differences in linear polarization sensitivity with HAM side are as high as ~0.13 %, compared to up to ~1.0 % for JPSS-1 VIIRS.
- Large detector-to-detector and scan angle differences were observed within bands (up to ~2 % in M1). This is likely the result of angle of incidence changes on the filter assembly. The JPSS-1 VIIRS results showed much higher variability for some bands.
- Comparisons between test configurations in general agreed (using the BVONIR polarizer sheet with and without the Sonoma shaping filter).
- Band maximum uncertainties range from 0.11 % (for M6) to 0.43 % (for M1), which is comparable to JPSS-1 VIIRS. All bands are well below the specified maximum uncertainty of 0.5 %.
- The largest uncertainty contributors are the source stability, efficiency, SIS – TOA, and test setup uncertainties; the largest single contributor for any band is the SIS – TOA uncertainty of 0.39 % for M1.

Table 1: Specified maximum polarization sensitivity [5]

Band	Sensitivity [%]
I2, M1, M7	3
I1, M2, M3, M4, M5, M6	2.5

Table 2: Data used in the FP-11 test analysis using the BVONIR polarizer without the Sonoma filter. Data for which the source was unstable are highlighted in red.

Test Type	UAID	Collects	Scan Angle	Samples	Lamps
Stray light – dark	4400831	1 – 25	-8	1616 – 1635	BH
Stray light – lollipop	4400834	1 – 25	-8	1616 – 1635	BH
Efficiency	4400836	1 – 25	-8	1616 – 1635	BH
Polarization Sensitivity	4400842	1 – 25	-8	1616 – 1635	BH
	4400845	1 – 25	55	1966 – 1985	BH
	4400849	1 – 25	-55	44 – 63	BH
	4400852	1 – 25	-45	598 – 617	BH
	4400856	1 – 25	-37	1040 – 1059	BH
	4400859	1 – 25	-30	1438 – 1457	BH
	4400862	1 – 25	-20	932 – 951	BH
	4400865	1 – 25	-15	1215 – 1234	BH
	4400869	1 – 25	-8	1612 – 1631	BH
	4400874	1 – 25	-15	1228 – 1247	CJ
	4400878	1 – 25	4	1220 – 1239	CJ
	4400881	1 – 25	22	1174 – 1193	CJ
	4400884	1 – 25	45	1415 – 1434	CJ
	4400886	1 – 25	-8	1610 – 1629	CJ
	4400888	1 – 25	-20	937 – 956	CJ

Table 3: Data used in the FP-11 test analysis using the BVO777 polarizer without the Sonoma filter.

Test Type	UAID	Collects	Scan Angle	Samples	Lamps
Efficiency	4400837	1 – 25	-8	1616 – 1635	BH
Polarization Sensitivity	4400841	1 – 25	-8	1616 – 1635	BH

Table 4: Data used in the FP-11 test analysis using the BVONIR polarizer with the Sonoma filter. Data for which the source was unstable are highlighted in red.

Test Type	UAID	Collects	Scan Angle	Samples	Lamps
Stray light – dark	4400830	1 – 25	-8	1625 – 1654	BH
Stray light – lollipop	4400833	1 – 25	-8	1625 – 1654	BH
Efficiency	4400835	1 – 25	-8	1616 – 1635	BH
Polarization Sensitivity	4400839	1 – 25	-8	1616 – 1635	BH
	4400844	1 – 25	55	1966 – 1985	BH
	4400847	1 – 25	-55	44 – 63	BH
	4400851	1 – 25	-45	598 – 617	BH
	4400853	1 – 25	-37	1040 – 1059	BH
	4400858	1 – 25	-30	1438 – 1457	BH
	4400860	1 – 25	-20	932 – 951	BH
	4400864	1 – 25	-15	1215 – 1234	BH
	4400870	1 – 25	-8	1612 – 1631	CJ
	4400873	1 – 25	-15	1228 – 1247	CJ
	4400877	1 – 25	4	1220 – 1239	CJ
	4400880	1 – 25	22	1174 – 1193	CJ
	4400883	1 – 25	45	1415 – 1434	CJ
	4400885	1 – 25	-8	1610 – 1629	CJ
	4400887	1 – 25	-20	937 – 956	CJ

Table 5: Data used in the FP-11 test analysis using the BVO777 polarizer with the Sonoma filter.

Test Type	UAID	Collects	Scan Angle	Samples	Lamps
Efficiency	4400838	1 – 25	-8	1616 – 1635	BH
Polarization Sensitivity	4400840	1 – 25	-8	1616 – 1635	BH

Table 6: Maximum polarization factors (a_2) for HAM side 0.

Band	Sensor	Scan Angle										
		-55	-45	-37	-30	-20	-15	-8	4	22	45	55
I1	SNPP	1.50	1.24	~	~	0.93	~	0.85	~	0.70	0.64	0.62
	J1	0.81	0.74	0.76	0.73	0.73	0.73	0.78	0.76	0.82	0.84	0.85
	J2	0.81	0.80	0.81	0.85	0.85	0.86	0.86	0.86	0.85	0.87	0.87
I2	SNPP	0.27	0.29	~	~	0.34	~	0.37	~	0.47	0.51	0.51
	J1	0.73	0.62	0.55	0.46	0.36	0.36	0.43	0.50	0.50	0.61	0.66
	J2	1.14	1.03	0.97	1.03	1.10	1.14	1.19	1.26	1.33	1.41	1.44
M1	SNPP	2.99	2.63	~	~	1.95	~	1.79	~	1.42	1.21	1.40
	J1	5.12	5.26	5.37	5.48	5.54	5.57	5.63	5.69	5.65	5.50	5.37
	J2	4.22	4.25	4.33	4.43	4.59	4.63	4.70	4.81	4.83	4.70	4.54
M2	SNPP	2.11	1.97	~	~	1.63	~	1.53	~	1.28	1.17	1.29
	J1	3.72	3.79	3.88	3.91	3.90	3.91	3.94	3.95	3.89	3.96	4.02
	J2	1.76	1.53	1.44	1.39	1.34	1.34	1.32	1.32	1.50	1.70	1.74
M3	SNPP	1.20	1.14	~	~	0.90	~	0.82	~	0.61	0.70	0.80
	J1	2.89	2.85	2.86	2.81	2.73	2.71	2.68	2.63	2.62	2.79	2.82
	J2	1.17	1.02	0.97	0.94	0.91	0.90	0.92	1.01	1.14	1.27	1.30
M4	SNPP	1.05	1.10	~	~	1.19	~	1.16	~	1.00	0.88	0.84
	J1	3.61	3.90	4.09	4.15	4.16	4.21	4.19	4.17	4.04	3.88	3.79
	J2	0.90	0.94	0.98	1.04	1.09	1.10	1.12	1.15	1.15	1.12	1.07
M5	SNPP	1.19	1.02	~	~	0.85	~	0.84	~	0.76	0.73	0.69
	J1	1.90	1.86	1.89	1.85	1.82	1.84	1.80	1.82	1.81	1.80	1.80
	J2	1.50	1.60	1.58	1.60	1.57	1.58	1.55	1.52	1.53	1.52	1.50
M6	SNPP	0.99	0.96	~	~	0.94	~	0.94	~	0.88	0.82	0.76
	J1	1.61	1.32	1.13	1.00	0.86	0.85	0.79	0.74	0.73	0.74	0.76
	J2	1.44	1.20	1.05	0.96	0.90	0.88	0.85	0.84	0.85	0.86	0.86
M7	SNPP	0.17	0.19	~	~	0.25	~	0.28	~	0.38	0.42	0.41
	J1	0.73	0.62	0.54	0.46	0.36	0.36	0.32	0.38	0.44	0.55	0.60
	J2	1.07	0.96	0.89	0.85	0.91	0.94	0.98	1.04	1.12	1.19	1.23
DNB LGS	SNPP	1.37	1.29	~	~	1.12	~	1.07	~	0.97	0.93	0.91
	J1	1.66	1.60	1.54	1.44	1.41	1.42	1.41	1.37	1.36	1.38	1.37
	J2	1.79	1.70	1.62	1.57	1.56	1.55	1.54	1.54	1.54	1.58	1.57

Table 7: Maximum polarization factors (a_2) for HAM side 1.

Band	Sensor	Scan Angle										
		-55	-45	-37	-30	-20	-15	-8	4	22	45	55
I1	SNPP	0.86	0.76	~	~	0.62	~	0.59	~	0.54	0.58	0.61
	J1	0.86	0.90	0.94	0.94	0.94	0.97	0.95	0.97	1.00	1.03	1.03
	J2	0.82	0.80	0.80	0.84	0.83	0.85	0.85	0.85	0.84	0.85	0.85
I2	SNPP	0.49	0.45	~	~	0.47	~	0.51	~	0.56	0.56	0.55
	J1	1.19	0.92	0.76	0.62	0.50	0.49	0.48	0.50	0.53	0.58	0.61
	J2	1.05	0.98	0.93	1.01	1.10	1.14	1.19	1.27	1.35	1.43	1.46
M1	SNPP	3.14	2.73	~	~	2.01	~	1.83	~	1.45	1.23	1.39
	J1	5.57	5.73	5.88	6.01	6.17	6.17	6.20	6.31	6.41	6.16	5.95
	J2	4.16	4.20	4.30	4.40	4.51	4.58	4.63	4.72	4.74	4.64	4.48
M2	SNPP	2.25	2.05	~	~	1.65	~	1.54	~	1.28	1.17	1.30
	J1	4.08	4.08	4.15	4.19	4.18	4.20	4.23	4.25	4.19	4.34	4.45
	J2	1.66	1.47	1.39	1.35	1.31	1.31	1.30	1.30	1.47	1.65	1.68
M3	SNPP	1.45	1.31	~	~	0.96	~	0.85	~	0.62	0.71	0.81
	J1	2.92	2.86	2.86	2.82	2.76	2.76	2.75	2.74	2.85	3.06	3.09
	J2	1.11	0.98	0.94	0.92	0.89	0.89	0.91	1.00	1.12	1.25	1.28
M4	SNPP	1.59	1.52	~	~	1.37	~	1.30	~	1.02	0.86	0.82
	J1	4.03	4.20	4.33	4.34	4.32	4.34	4.31	4.28	4.15	3.99	3.90
	J2	0.87	0.92	0.96	1.03	1.09	1.10	1.11	1.15	1.14	1.11	1.06
M5	SNPP	0.81	0.74	~	~	0.70	~	0.69	~	0.61	0.59	0.57
	J1	2.10	2.17	2.20	2.18	2.13	2.13	2.13	2.07	2.02	1.99	1.97
	J2	1.60	1.57	1.55	1.57	1.55	1.55	1.52	1.51	1.52	1.51	1.48
M6	SNPP	1.29	1.14	~	~	0.96	~	0.92	~	0.81	0.75	0.70
	J1	1.03	0.92	0.89	0.86	0.86	0.90	0.91	0.94	0.95	0.95	0.94
	J2	1.49	1.24	1.08	0.99	0.91	0.88	0.85	0.84	0.84	0.84	0.84
M7	SNPP	0.52	0.47	~	~	0.43	~	0.44	~	0.48	0.47	0.45
	J1	1.18	0.92	0.74	0.61	0.48	0.47	0.44	0.45	0.47	0.52	0.56
	J2	1.00	0.91	0.85	0.84	0.91	0.94	0.99	1.05	1.13	1.21	1.24
DNB LGS	SNPP	1.35	1.25	~	~	1.06	~	1.00	~	0.95	0.93	0.93
	J1	1.44	1.42	1.42	1.36	1.39	1.43	1.44	1.46	1.51	1.57	1.59
	J2	1.80	1.70	1.62	1.58	1.56	1.55	1.53	1.53	1.52	1.55	1.54

Table 8: Maximum uncertainty on polarization factors (a_2) over detectors, HAM sides, and scan angles [in %].

	I1	I2	M1	M2	M3	M4	M5	M6	M7
Noise	0.00	0.00	0.00	0.00	0.00	0.01	0.00	0.00	0.00
Source stability	0.14	0.01	0.01	0.02	0.01	0.25	0.08	0.01	0.01
Stray light	0.01	0.00	0.00	0.00	0.00	0.04	0.01	0.00	0.00
Sheet angle	0.00	0.00	0.02	0.01	0.00	0.00	0.00	0.00	0.00
Efficiency	0.10	0.01	0.07	0.16	0.11	0.21	0.09	0.01	0.01
Measurement total	**0.17**	**0.01**	**0.07**	**0.16**	**0.11**	**0.33**	**0.12**	**0.02**	**0.02**
Repeatability	0.05	0.05	0.05	0.04	0.03	0.06	0.06	0.04	0.04
Scan angle interpolation	0.05	0.07	0.05	0.06	0.03	0.03	0.05	0.05	0.07
SIS – TOA	0.08	0.03	0.39	0.05	0.13	0.05	0.09	0.01	0.03
OOB	0.00	0.00	0.09	0.03	0.01	0.00	0.00	0.00	0.00
Test setup	0.20	0.10	0.14	0.12	0.14	0.10	0.13	0.09	0.10
JPSS-2	**0.27**	**0.13**	**0.43**	**0.21**	**0.21**	**0.35**	**0.19**	**0.11**	**0.13**
JPSS-1	**0.22**	**0.13**	**0.37**	**0.14**	**0.21**	**0.13**	**0.18**	**0.13**	**0.13**
Specification	**0.50**	**0.50**	**0.50**	**0.50**	**0.50**	**0.50**	**0.50**	**0.50**	**0.50**

Figure 1: Schematic of the polarization sensitivity test setup

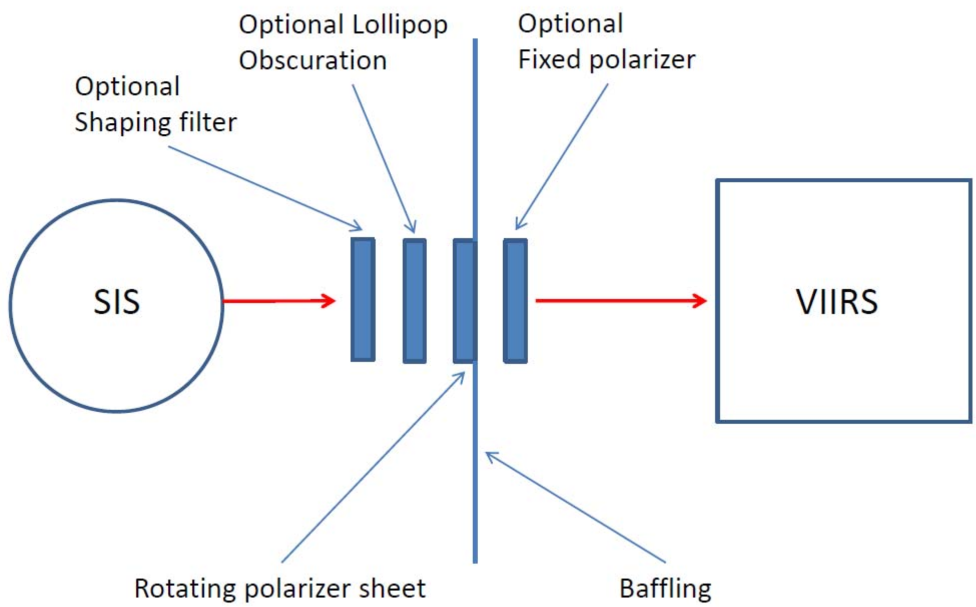

Figure 2: Schematic of the view of BVONIR polarizer from VIIRS with VIIRS coordinate system

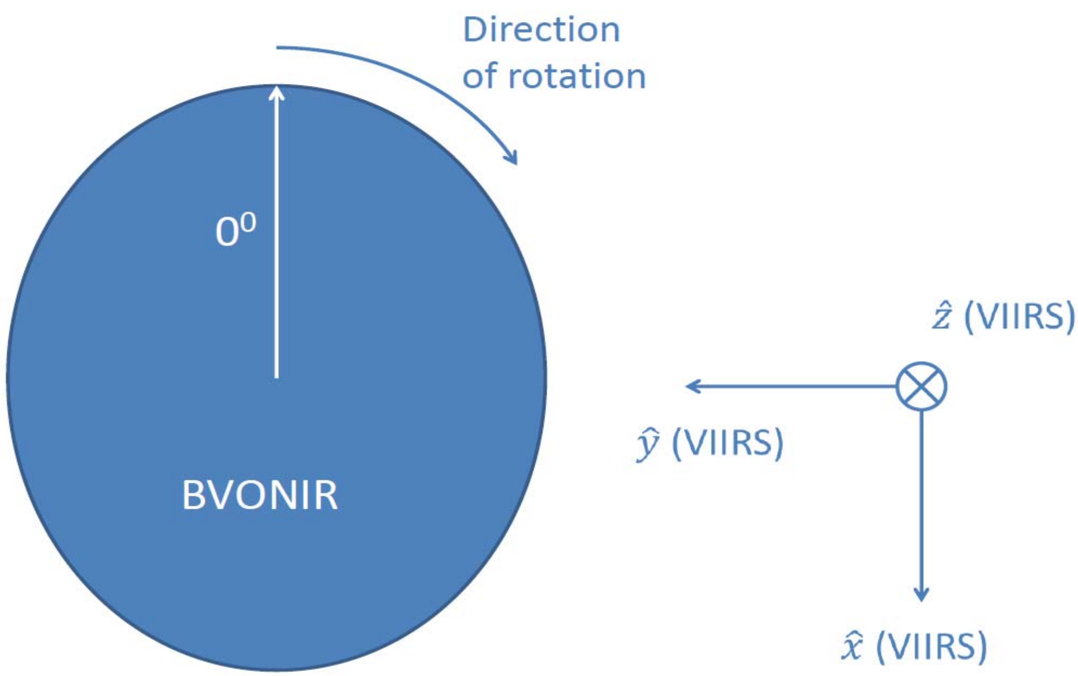

Figure 3: Radiance monitor data tracking the output of the SIS-100-2 (BVONIR with the Sonoma filter)

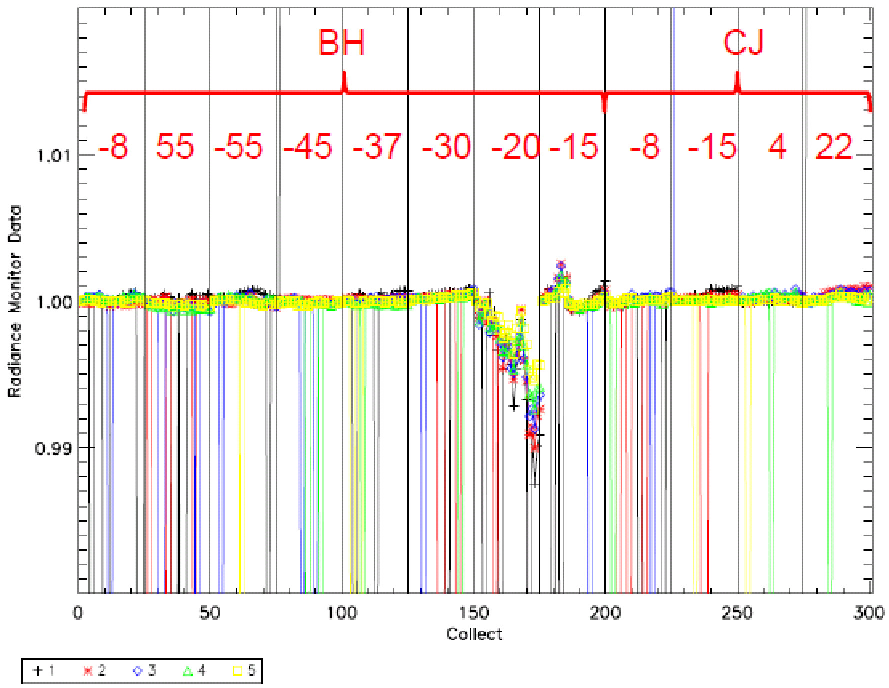

Figure 4: Radiance monitor data tracking the output of the SIS-100-2 (BVONIR with the Sonoma filter)

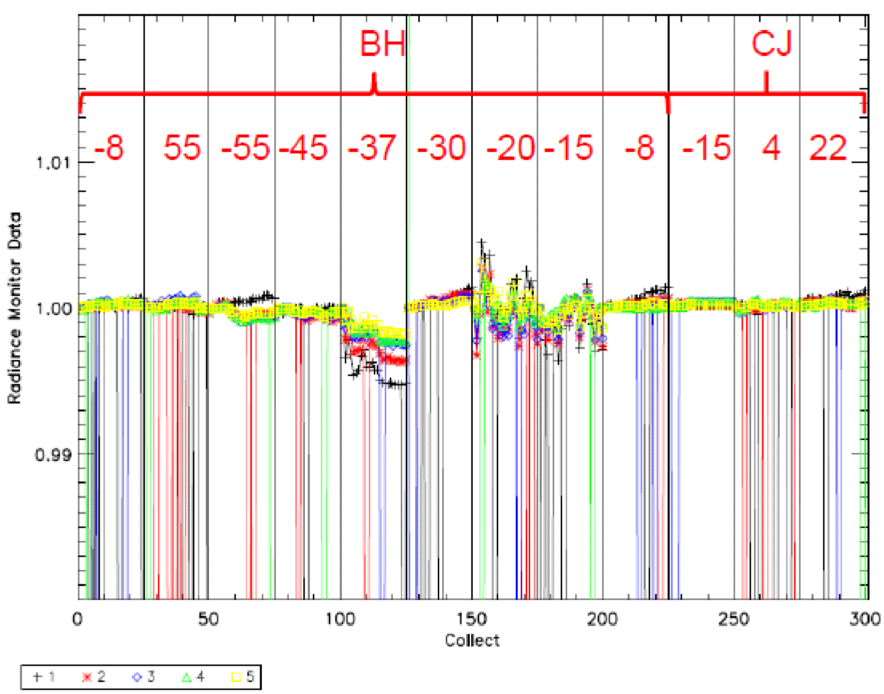

Figure 5: Uncertainty tree for the polarization factor a_2

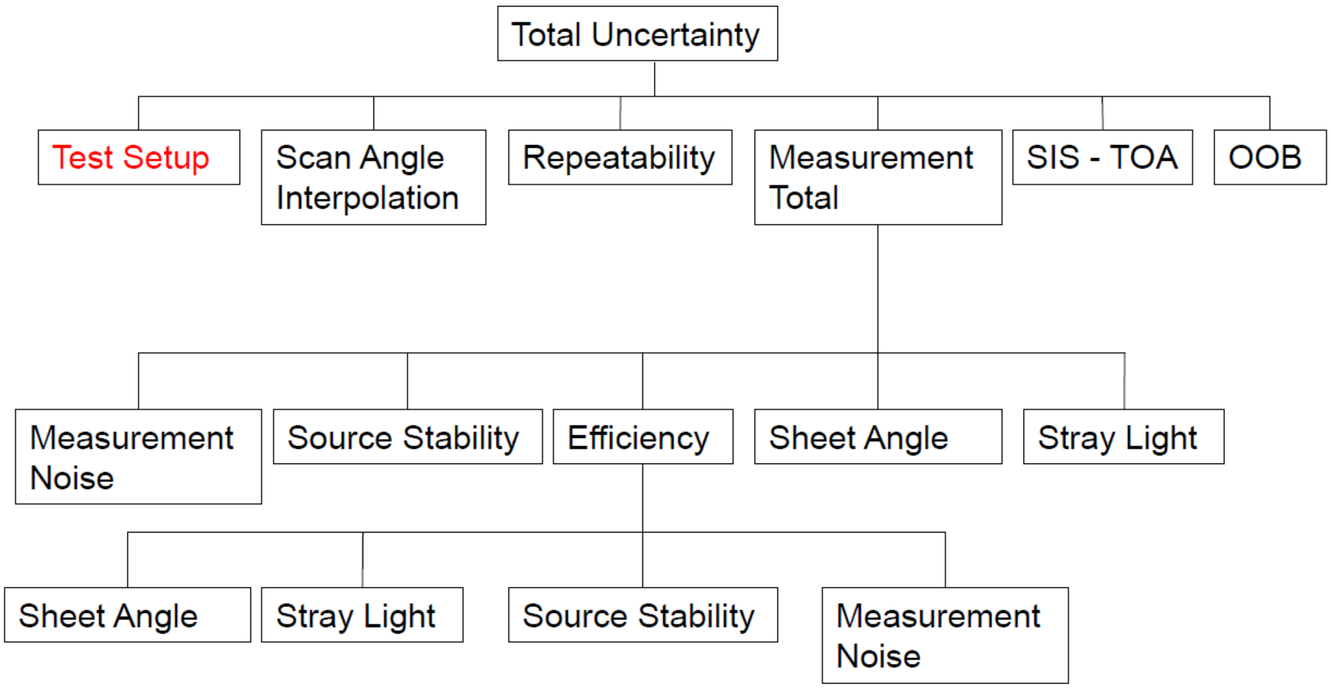

Figure 6: Stray light observed in M7 HAM 0 using the BVONIR polarizer (no Sonoma filter) with the source dark

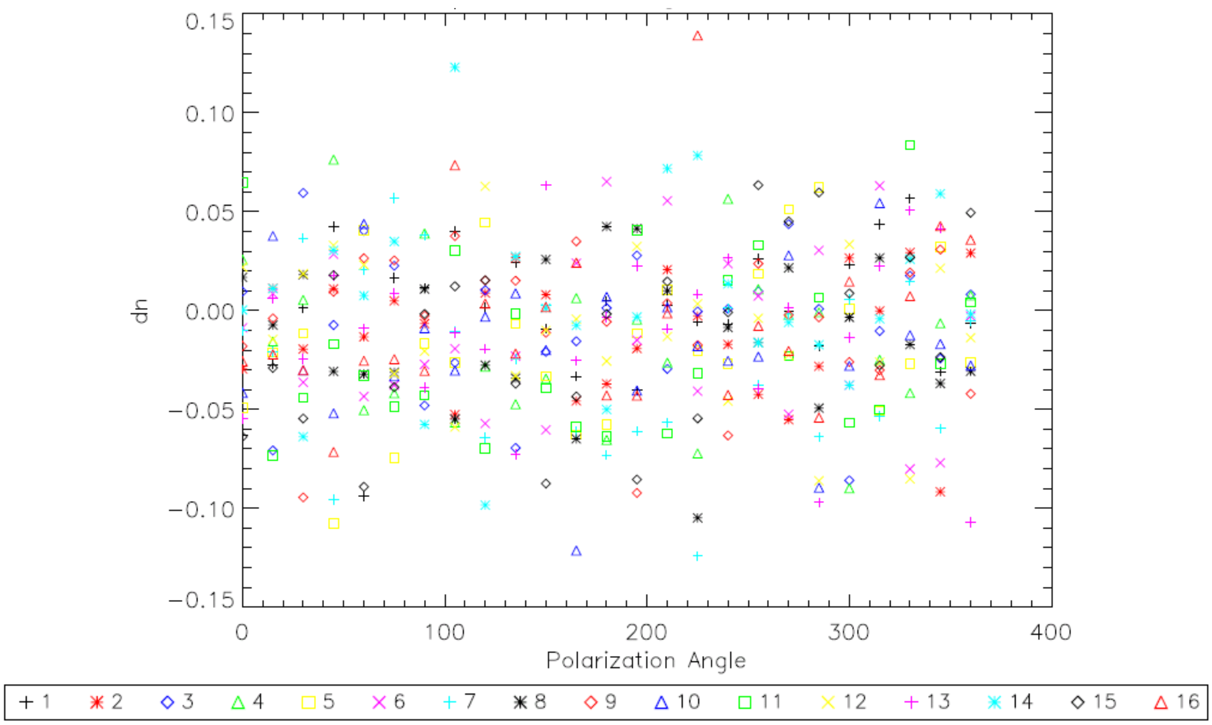

Figure 7: Stray light observed in M7 HAM A using the BVONIR polarizer (no Sonoma filter) with the lollipop obscuration

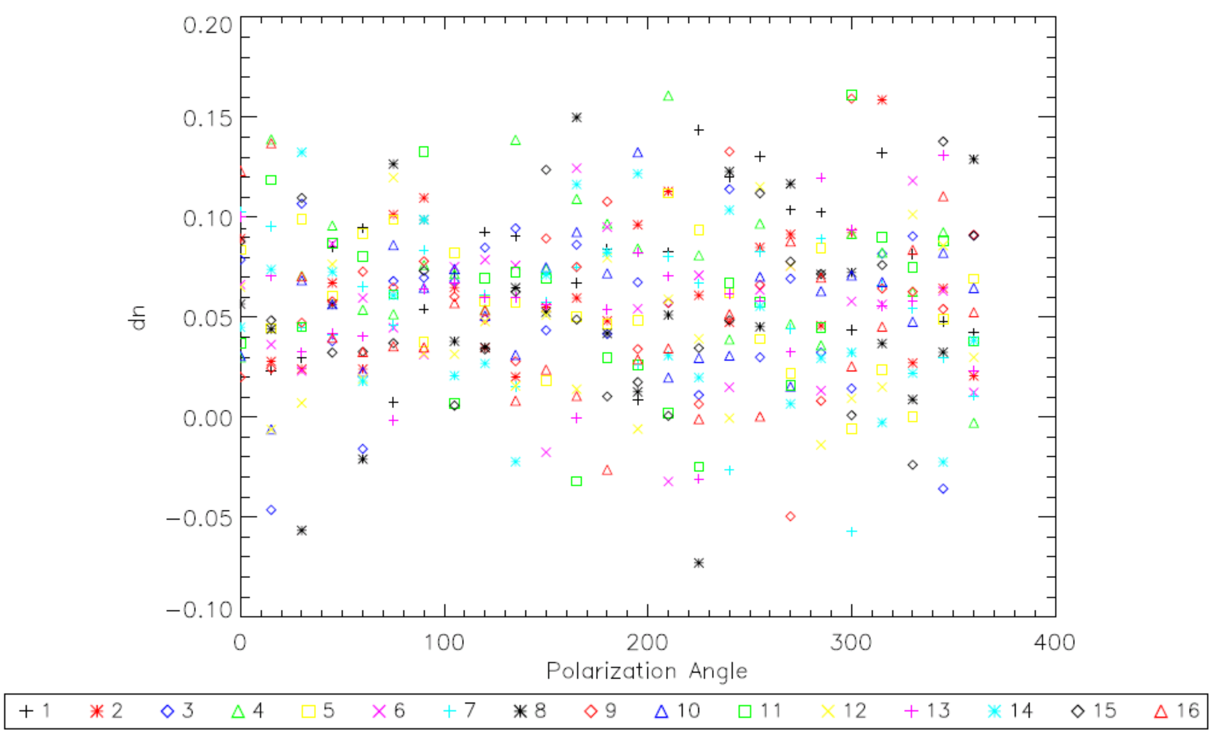

Figure 8: Band average FP-11 BVONIR polarizer efficiencies determined with and without the Sonoma filter

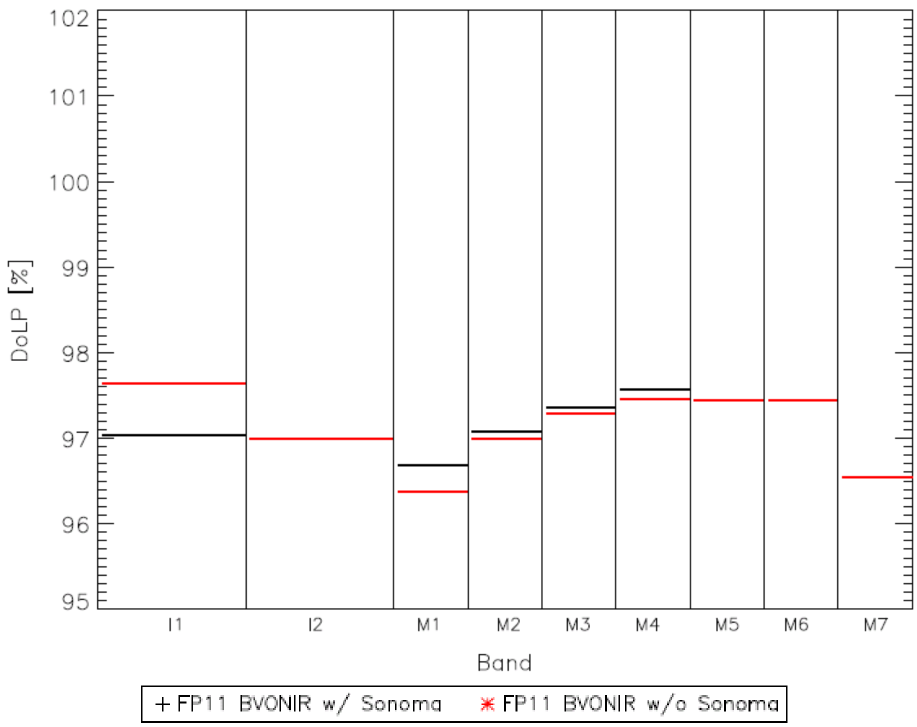

Figure 9: dn as a function of polarizer angle for M7 HAM 0 using BVONIR without the Sonoma filter (-8 degrees scan angle)

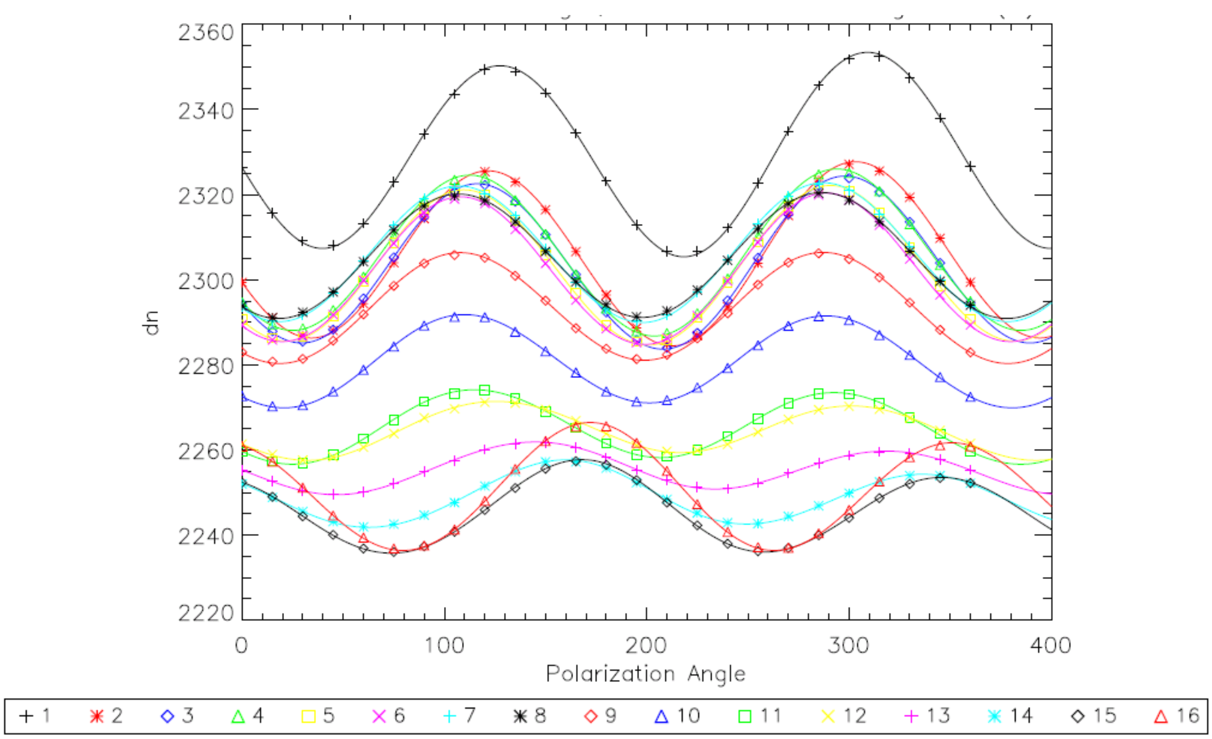

Figure 10: Fourier coefficients for M7 HAM 0 using BVONIR without the Sonoma filter

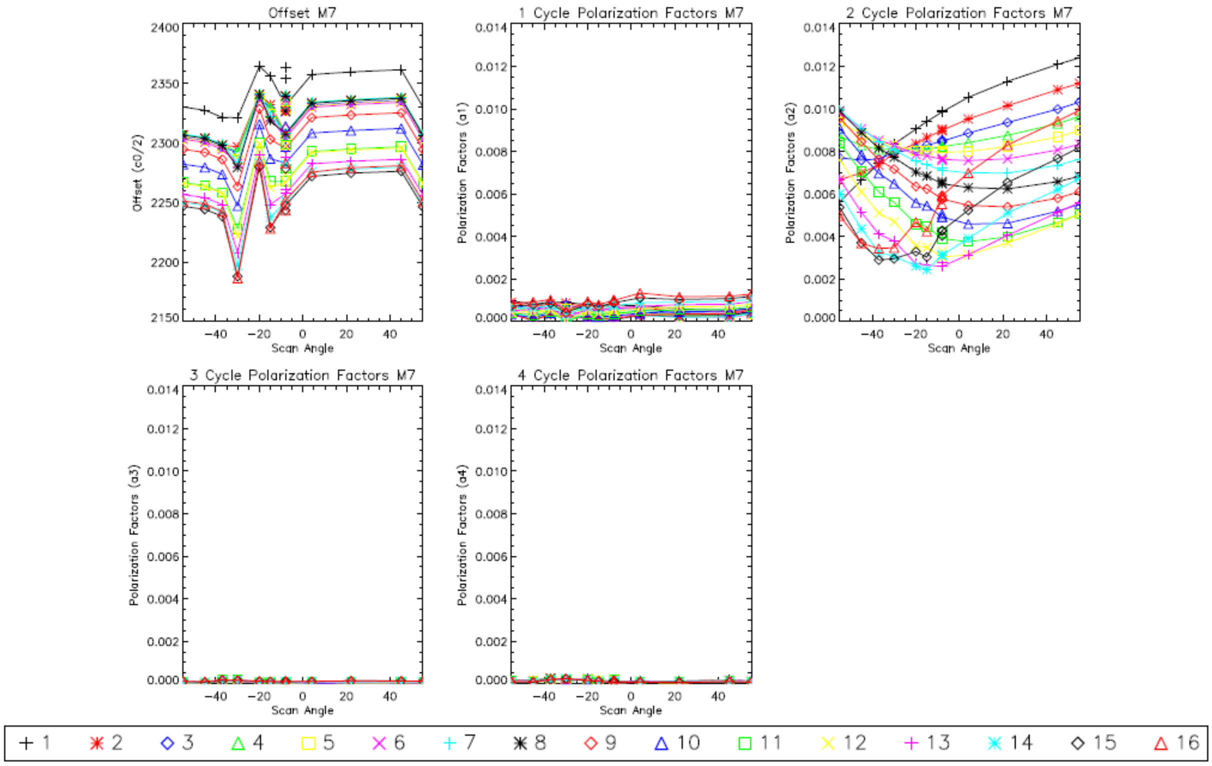

Figure 11: Polarization factor a_2 for M1, HAM side 0 in [%] across test configurations and repeated measurements

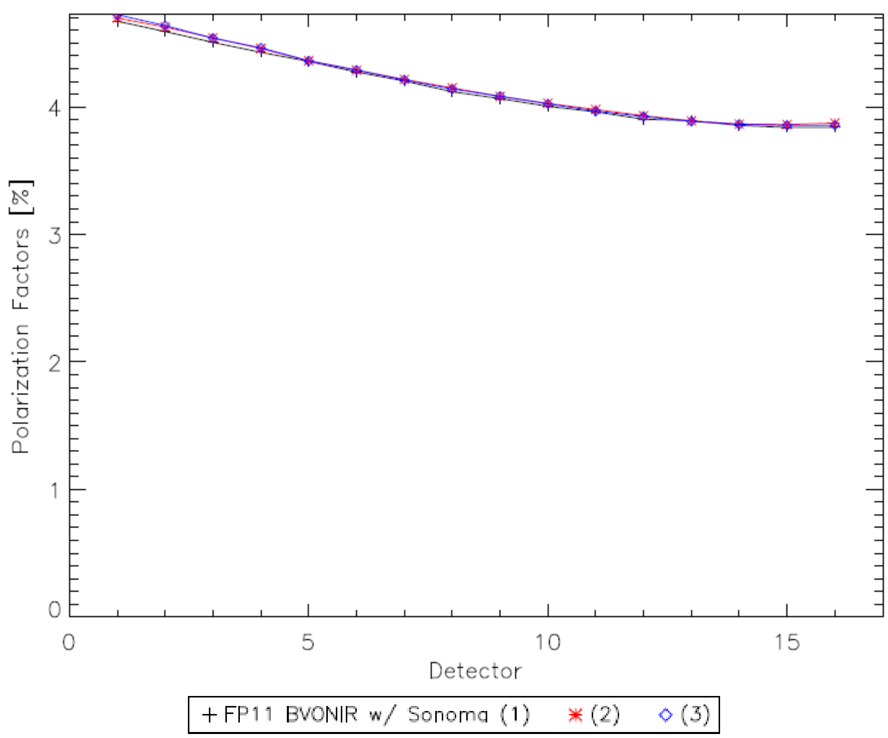

Figure 12: Polarization factor a_2 for HAM side 0 in [%] across scan angles

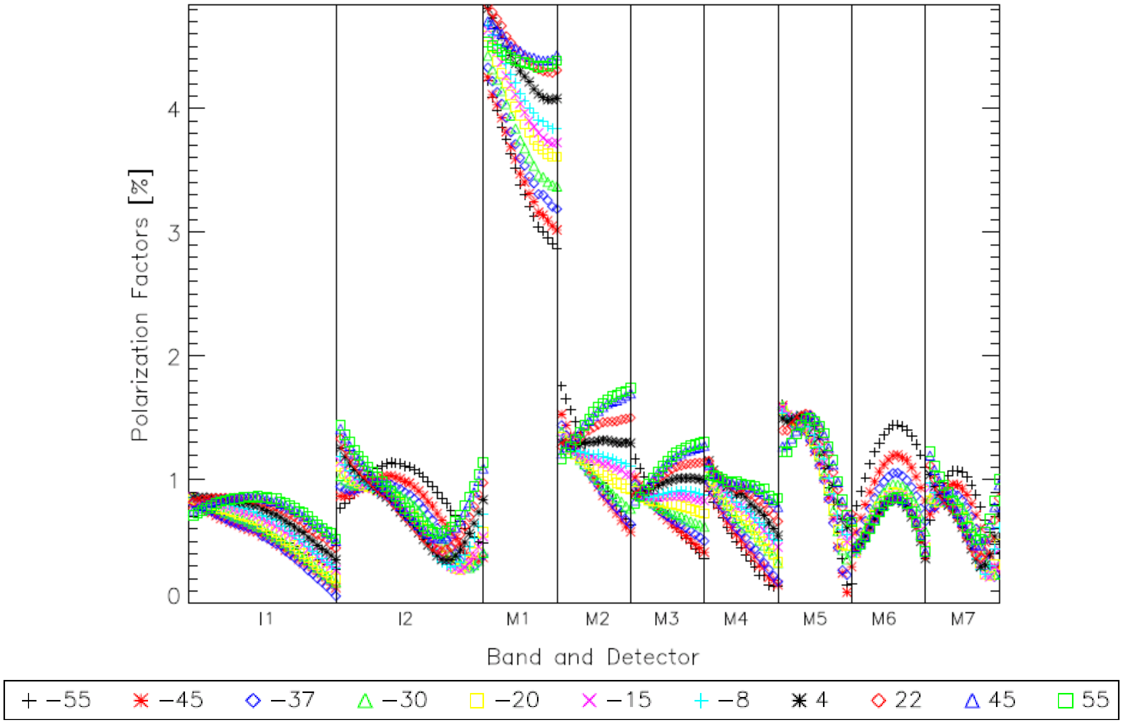

Figure 13: Polarization factor a_2 for HAM side 1 in [%] across scan angles

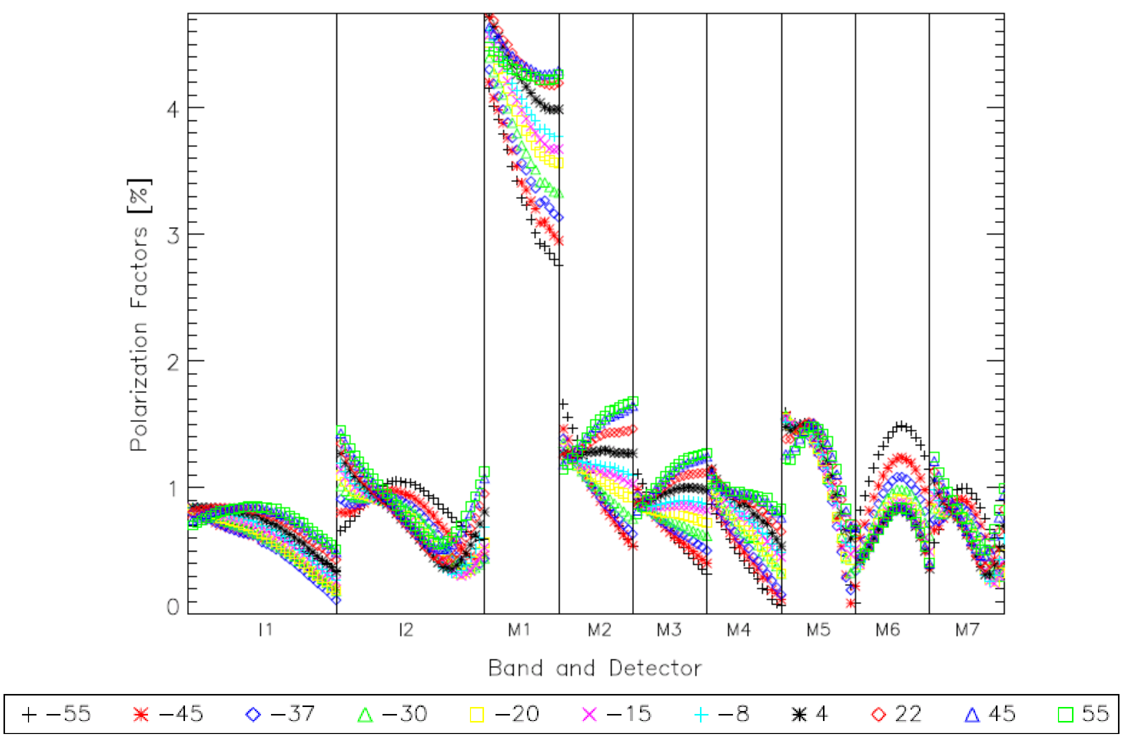

Figure 14: Polarization phase δ_2 for HAM side 0 in [radians] across scan angles

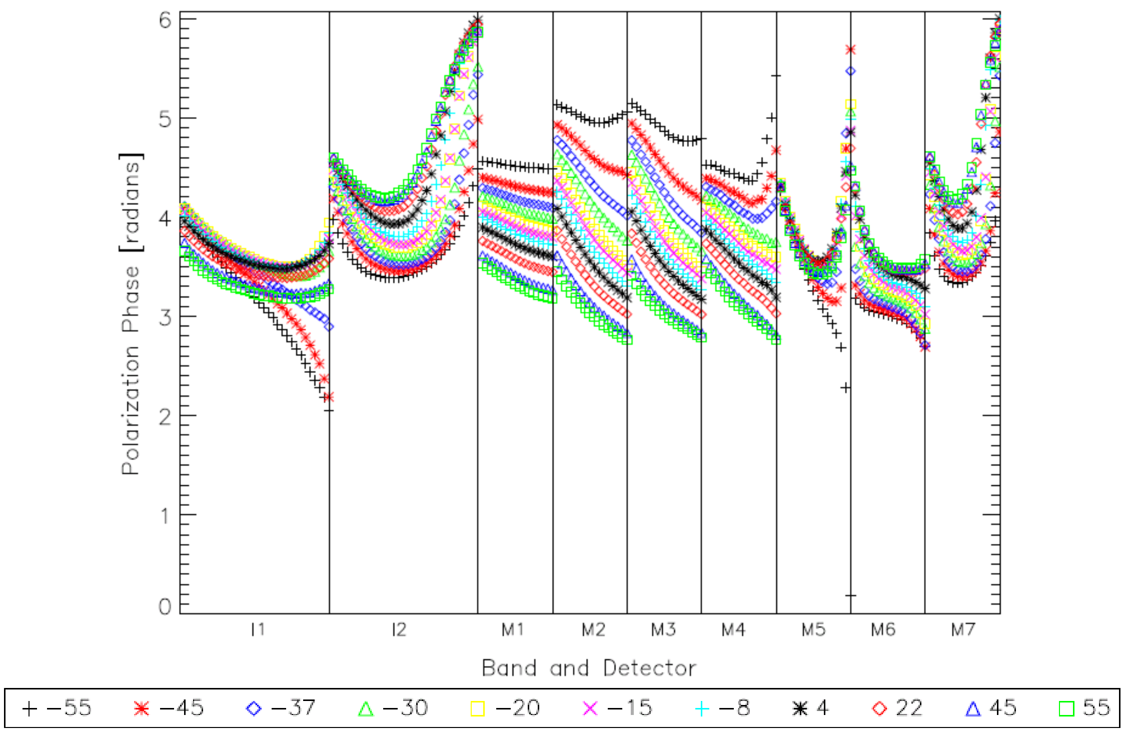

Figure 15: Polarization phase δ_2 for HAM side 1 in [radians] across scan angles

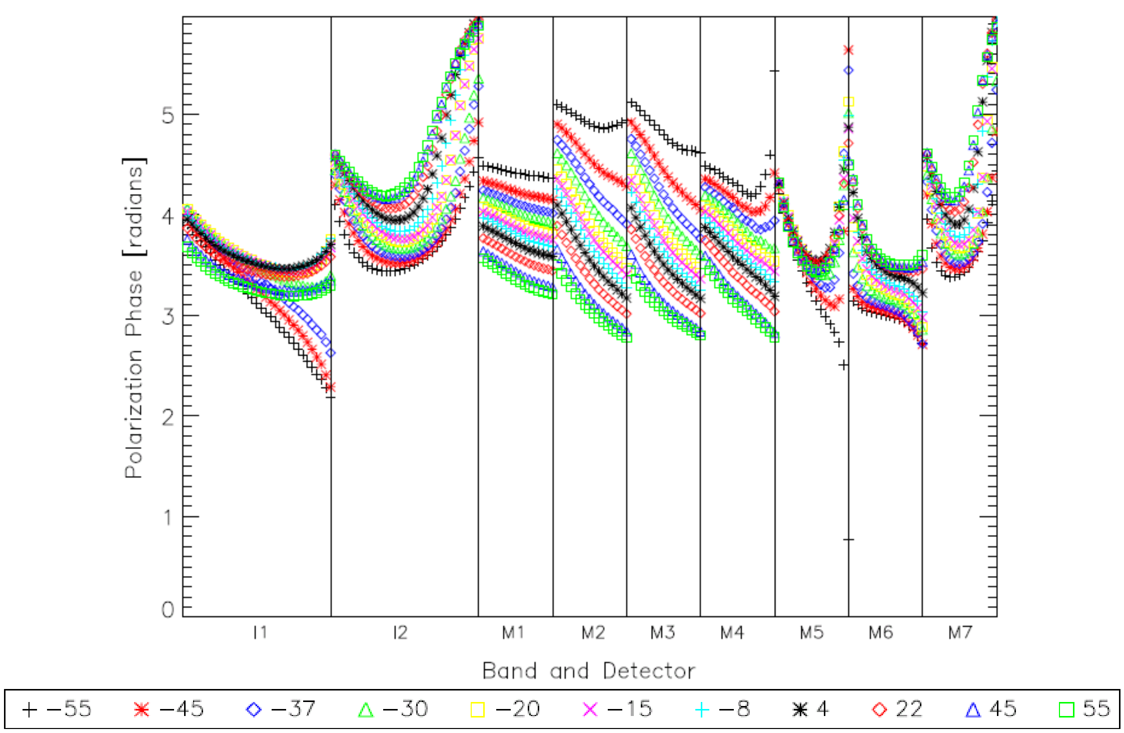

Figure 16: Polarization factor a2 for DNB LGS, HAM side 0 in [%] across test configurations and scan angles

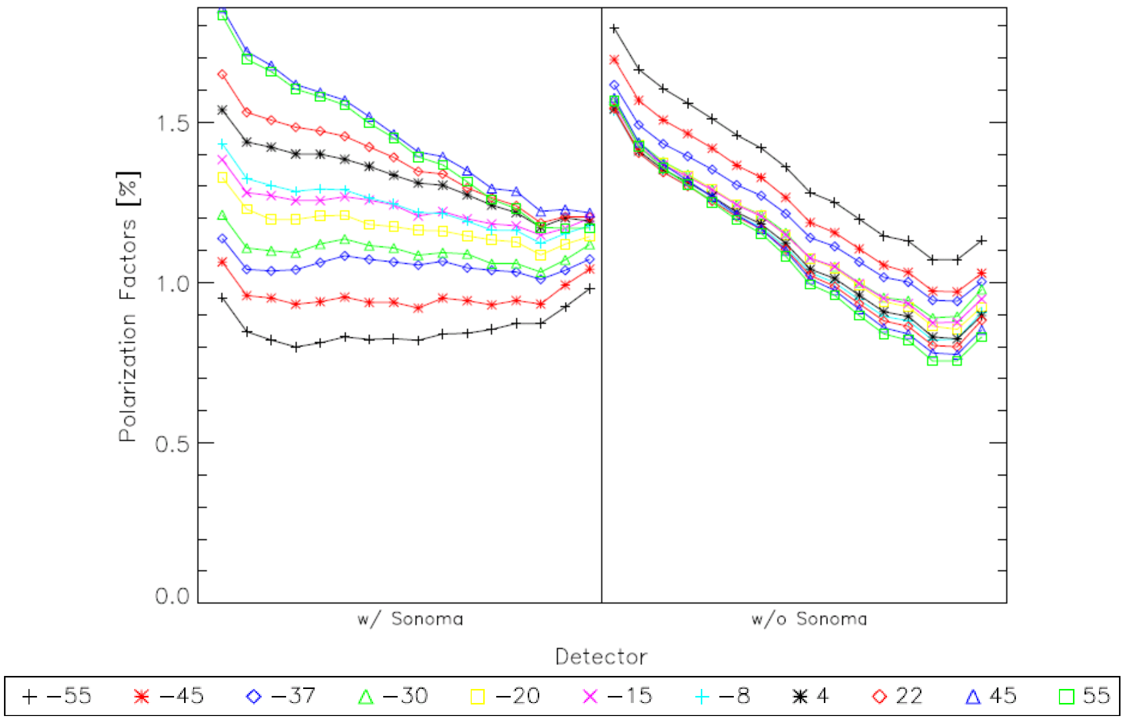

Figure 17: Polarization factor a2 for DNB LGS, HAM side 0 in [%] across test configurations and scan angles

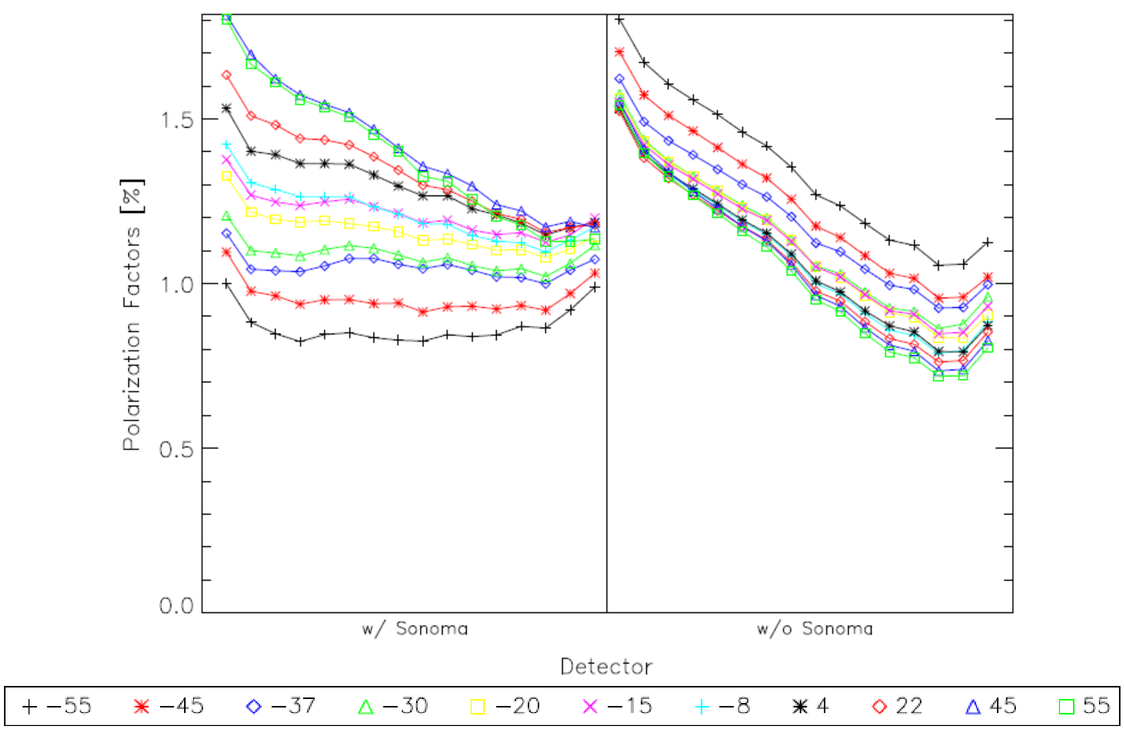

Figure 18: Polarization factor δ_2 for DNB LGS, HAM side 0 in [radians] across test configurations and scan angles

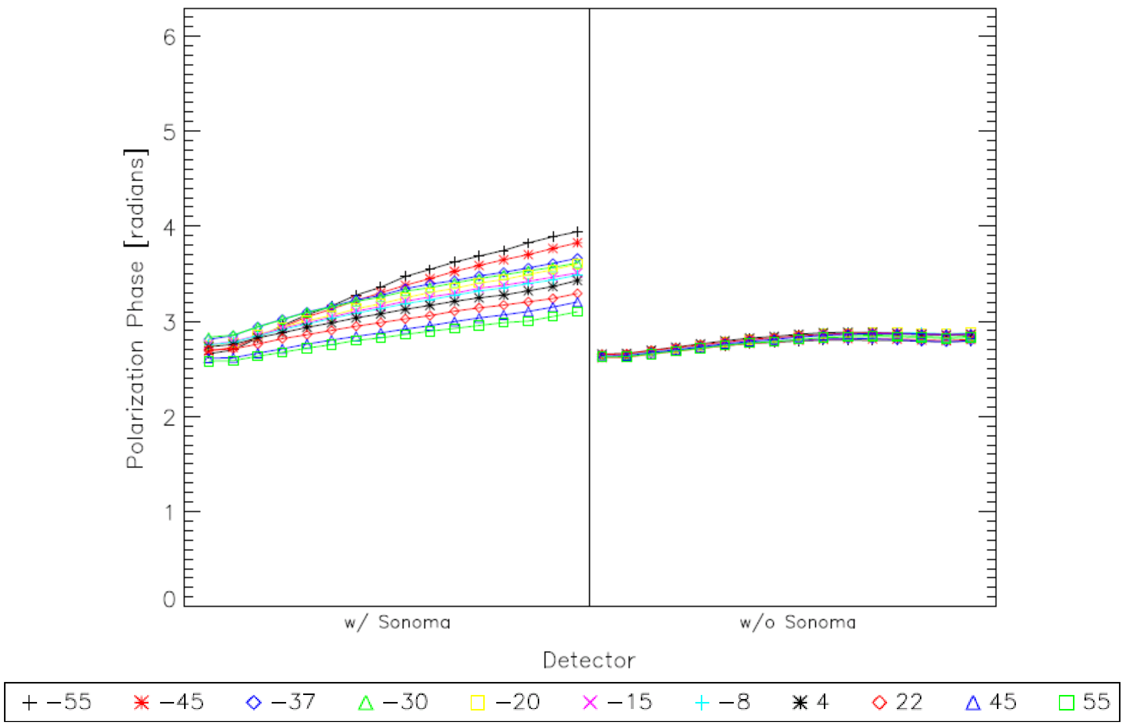

Figure 19: Polarization factor δ_2 for DNB LGS, HAM side 0 in [radians] across test configurations and scan angles